# REPORT DOCUMENTATION PAGE

Form Approved OMB NO. 0704-0188

The public reporting burden for this collection of information is estimated to average 1 hour per response, including the time for reviewing instructions, searching existing data sources, gathering and maintaining the data needed, and completing and reviewing the collection of information. Send comments regarding this burden estimate or any other aspect of this collection of information, including suggesstions for reducing this burden, to Washington Headquarters Services, Directorate for Information Operations and Reports, 1215 Jefferson Davis Highway, Suite 1204, Arlington VA, 22202-4302. Respondents should be aware that notwithstanding any other provision of law, no person shall be subject to any oenalty for failing to comply with a collection of information if it does not display a currently valid OMB control number.
PLEASE DO NOT RETURN YOUR FORM TO THE ABOVE ADDRESS.

| 1. REPORT DATE (DD-MM-YYYY) | 2. REPORT TYPE | 3. DATES COVERED (From - To) |
|---|---|---|
| | New Reprint | - |

**4. TITLE AND SUBTITLE**

Characterization of Meander Dipole Antennas With a Geometry-Based, Frequency-Independent Lumped Element Model

**5a. CONTRACT NUMBER**

**5b. GRANT NUMBER**

W911NF-04-D-0001

**5c. PROGRAM ELEMENT NUMBER**

611102

**6. AUTHORS**

Olusola O. Olaode, W. Devereux Palmer, William T. Joines

**5d. PROJECT NUMBER**

**5e. TASK NUMBER**

**5f. WORK UNIT NUMBER**

**7. PERFORMING ORGANIZATION NAMES AND ADDRESSES**

Duke University
130 Hudson Hall, Box 90271
Duke University
Durham, NC 27705 -

**8. PERFORMING ORGANIZATION REPORT NUMBER**

**9. SPONSORING/MONITORING AGENCY NAME(S) AND ADDRESS(ES)**

U.S. Army Research Office
P.O. Box 12211
Research Triangle Park, NC 27709-2211

**10. SPONSOR/MONITOR'S ACRONYM(S)**

ARO

**11. SPONSOR/MONITOR'S REPORT NUMBER(S)**

49428-EL-SR.9

**12. DISTRIBUTION AVAILIBILITY STATEMENT**

Approved for public release; distribution is unlimited.

**13. SUPPLEMENTARY NOTES**

The views, opinions and/or findings contained in this report are those of the author(s) and should not contrued as an official Department of the Army position, policy or decision, unless so designated by other documentation.

**14. ABSTRACT**

Meander antennas have gained widespread use in applications such as Radio Frequency Identification (RFID) devices where space for the antenna is limited or a low-frequency operation is required. Several size reduction and synthesis methods have been proposed over time. However, few studies have focused on developing models to characterize the operation of meander antennas. In addition, existing models are frequency-dependent, which means that they are inherently narrowband. An alternative model that is based entirely on the geometry of a

**15. SUBJECT TERMS**

Dipole antennas, meander antenna, equivalent circuit, lumped elements

| 16. SECURITY CLASSIFICATION OF: | | | 17. LIMITATION OF ABSTRACT | 15. NUMBER OF PAGES | 19a. NAME OF RESPONSIBLE PERSON |
|---|---|---|---|---|---|
| a. REPORT | b. ABSTRACT | c. THIS PAGE | | | Dev Palmer |
| UU | UU | UU | UU | | 19b. TELEPHONE NUMBER: 919-549-4246 |

**Report Title**

Characterization of Meander Dipole Antennas With a Geometry-Based, Frequency-Independent Lumped Element Model

**ABSTRACT**

Meander antennas have gained widespread use in applications such as Radio Frequency Identification (RFID) devices where space for the antenna is limited or a low-frequency operation is required. Several size reduction and synthesis methods have been proposed over time. However, few studies have focused on developing models to characterize the operation of meander antennas. In addition, existing models are frequency-dependent, which means that they are inherently narrowband. An alternative model that is based entirely on the geometry of a Meander Dipole Antenna (MDA) and is frequency independent is proposed. To enhance the accuracy of the proposed model, the effect of mutual capacitances introduced through bending of the antenna wire is incorporated. The mutual capacitances are also a function of the antenna geometry. This model is expected to be more broadband relative to existing models. The equivalent circuit model proposed is validated through comparison with numerical simulations in EMCoS, a moment method-based software package. The discrepancies between predictions of the resonant frequencies of MDAs with our model and simulation results are found to be less than 3 %. Two classes of meander dipole antennas are introduced.

# REPORT DOCUMENTATION PAGE (SF298)
# (Continuation Sheet)

Continuation for Block 13

ARO Report Number 49428.9-EL-SR
Characterization of Meander Dipole Antennas W ...

Block 13: Supplementary Note
© 2012 . Published in IEEE Antennas and Wireless Propagation Letters, Vol. Ed. 0 11, (0) (2012), (, (0). DoD Components reserve a royalty-free, nonexclusive and irrevocable right to reproduce, publish, or otherwise use the work for Federal purposes, and to authroize others to do so (DODGARS §32.36). The views, opinions and/or findings contained in this report are those of the author(s) and should not be construed as an official Department of the Army position, policy or decision, unless so designated by other documentation.

Approved for public release; distribution is unlimited.

# Characterization of Meander Dipole Antennas With a Geometry-Based, Frequency-Independent Lumped Element Model

Olusola O. Olaode, *Member, IEEE*, W. Devereux Palmer, *Fellow, IEEE*, and William T. Joines, *Life Fellow, IEEE*

***Abstract*—Meander antennas have gained widespread use in applications such as radio frequency identification (RFID) devices where space for the antenna is limited or a low-frequency operation is required. Several size-reduction and synthesis methods have been proposed over time. However, few studies have focused on developing models to characterize the operation of meander antennas. In addition, existing models are frequency-dependent, which means that they are inherently narrowband. An alternative model that is based entirely on the geometry of a meander dipole antenna (MDA) and is frequency-independent is proposed. To enhance the accuracy of the proposed model, the effect of mutual capacitances introduced through bending of the antenna wire is incorporated. The mutual capacitances are also a function of the antenna geometry. This model is expected to be more broadband relative to existing models. The equivalent circuit model proposed is validated through comparison to numerical simulations in EMCoS, a moment-method-based software package. The discrepancies between predictions of the resonant frequencies of MDAs with our model and simulation results are found to be less than 3%. Two classes of meander dipole antennas are introduced.**

***Index Terms*—Dipole antennas, equivalent circuit, lumped elements, meander antenna.**

## I. Introduction

MEANDER antennas have been widely studied and applied since the concept was introduced by Rashed and Tai [1]. For applications where the antenna size is critical, meandering or folding an antenna wire increases its resonant length without the commensurate increase in its physical size. An example of such an application of meander antennas is in radio frequency identification (RFID) devices [2]–[4]. While much focus had been on the reconfiguration [5], [6] and optimization [4] of meander antennas for (physical) size reduction and impedance match reasons, it is also important to define broadband theoretical models in which structural changes are easily incorporated. Our focus will be on two classes of meander dipole antennas (MDA) that we have defined: Class 1 and Class 2. For a Class-1 MDA, the total length of the wire $L$ is kept constant while the height $H$ is allowed to vary. As each meander is introduced, the mutual capacitance in each meander section increases while the overall capacitance in the antenna structure decreases because the mutual capacitances in adjacent meander sections combine in series. As the number of bends $N$ increases, the overall capacitance of the antenna decreases while the inductance of the wire remains constant, and for a Class-1 MDA, we observe a consistent increase in the resonant frequency of the antenna with increasing $N$.

For a Class-2 MDA, the height $H$ of the antenna remains fixed while $L$ is allowed to increase as bends are added. As the length of wire increases, so does the total inductance. Although adding bends has a similar effect on the overall capacitance as described for a Class-1 MDA, the increase in inductance dominates, and for a Class-2 MDA, we observe a consistent decrease in the resonant frequency of the antenna with increasing $N$.

Meander dipole antennas were modeled and characterized previously by Endo *et al.* [7]. In [7], a center-fed meander dipole antenna was decomposed into short-terminated transmission-line sections. Each section was modeled with lumped elements (inductors) and analyzed with transmission-line equations. The resonant frequency of the MDA was predicted from the equation of the total inductance, i.e., self- and mutual inductance of the antenna wire. Best and Morrow [8] concluded that the inductive circuit representation of meander antennas, which does not account for the capacitance of the meander sections, is inaccurate in predicting the resonant frequency and does not accommodate geometrical changes in the antenna. The difference between our approach and the others mentioned previously is that we represent an MDA model adapted from the half-wave dipole model presented in [10] with lumped elements that are entirely a function of the antenna geometry rather than frequency, an approach that is inherently more broadband and more easily accommodates changes in geometry and configuration.

## II. Theoretical Analysis of the Meander Dipole Antenna Model

An MDA has many similarities to its straight dipole counterpart. Nakano [9] found the radiation patterns to be similar. Fig. 1(a) shows the familiar cosine current distribution on one-half of a straight dipole antenna (SDA). The current is maximum at the feed point and diminishes to zero at the antenna tip. In Fig. 1(b), the horizontal segments $w$ of the MDA do not contribute significantly to the radiated fields, but are part

Manuscript received February 16, 2012; accepted March 08, 2012. Date of publication March 19, 2012; date of current version April 09, 2012. This work was supported in part by the US Army Research Laboratory and the US Army Research Office under Agreement Number W911NF-04-D-0001, Delivery Order 0003.

O. O. Olaode and W. T. Joines are with the Department of Electrical and Computer Engineering, Duke University, Durham, NC 27708 USA (e-mail: olusola.olaode@duke.edu; william.joines@duke.edu).

W. D. Palmer is with the Electronics Division, Engineering Sciences Directorate, US Army Research Office, Durham, NC 27709 USA (e-mail: william.d.palmer44.civ@mail.mil).

Color versions of one or more of the figures in this letter are available online at http://ieeexplore.ieee.org.

Digital Object Identifier 10.1109/LAWP.2012.2191380

1536-1225/$31.00 © 2012 IEEE

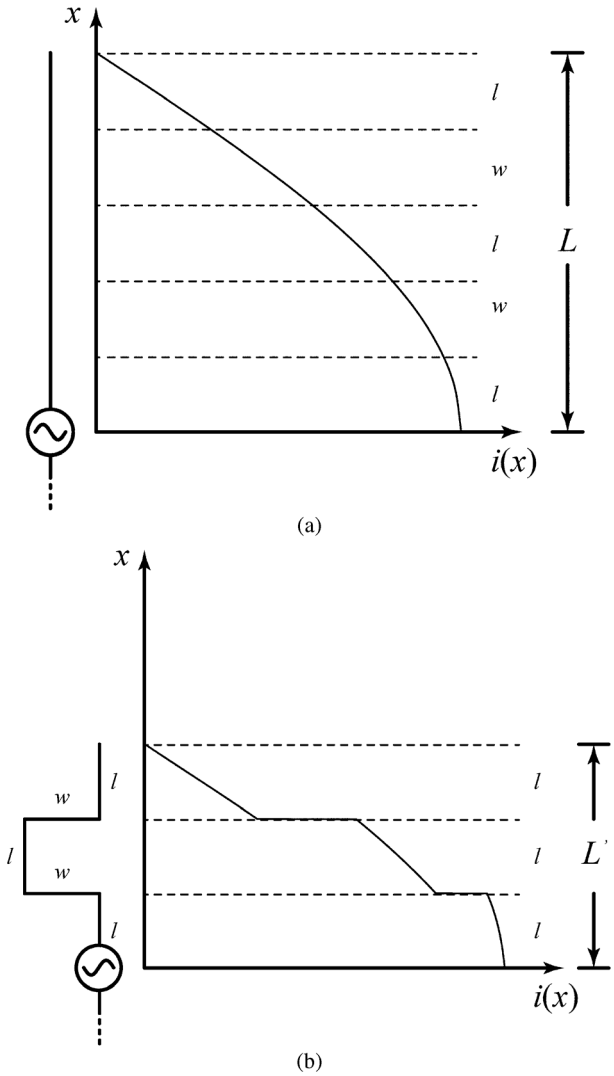


Fig. 1. (a) The familiar cosine current distribution on one half of an SDA is continuous from the feed point to the antenna tip. (b) The horizontal segments $w$ of the meander dipole antenna do not contribute to the radiated field, so the current distribution on the vertical segments $l$ forms a piecewise approximation of a cosine current distribution, only compacted into the smaller overall length.

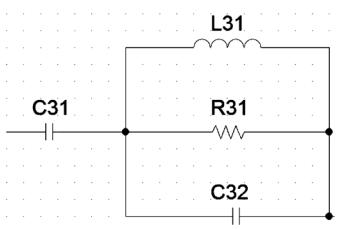


Fig. 2. Broadband equivalent circuit model from Tang *et al.* [11] used for both the SDA and the MDA.

of the overall electrical length of the MDA. As a result, the current distribution on the vertical sections $l$ of the MDA forms a piecewise representation of the current distribution on the SDA, only compacted into the smaller overall length. These similarities will be exploited later to create a frequency-independent, geometry-based MDA model.

Tang *et al.* [10] derived a four-element model (see Fig. 2) for a straight dipole antenna. The equations to calculate all the lumped elements were solely a function of the antenna geometry. Based

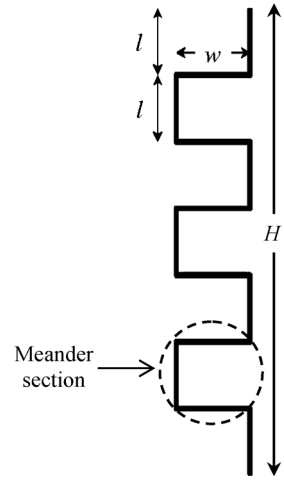


Fig. 3. One arm of a three-bend ($N = 3$) MDA. The total length of one arm of the wire is $L$ i.e. $L = (7l + 6w)$. $H$ is the height. For each $N$ considered, the lengths of all vertical segments, $l$ are equal. The lengths of all horizontal segments, $w$ are also equal.

on the MDA-SDA similarities identified previously, these equations can be adapted to MDAs as well. They are as follows:

$$C_{31} = \left\{ \frac{12.0674(L - 2wN)}{\log\left(\frac{2L-2wN}{a}\right) - 0.7245} \right\} pF \tag{1a}$$

$$C_{32} = 2(L - 2wN)\left\{ \frac{0.89075}{\left[\log\left(\frac{2(L-2wN)}{a}\right)\right]^{0.8006} - 0.861} - 0.02541 \right\} pF \tag{1b}$$

$$L_{31} = 0.2L\left\{ \begin{matrix} \left[1.4813 \log\left(\frac{2L}{a}\right)\right]^{1.012} \\ -0.6188 \end{matrix} \right\} \mu H \tag{1c}$$

where $N$ is the number of bends, $a$ is the radius of the wire, and $L$ is the total wire length of each arm of the MDA. In Fig. 3, $L = (7l + 6w)$. The equations for $C_{31}$ and $C_{32}$ do not consider the horizontal segments. The self-inductance of a wire remains relatively unchanged as long as the length of the horizontal segment, $w$, is electrically small. Therefore, $L_{31}$ is approximately equal to the self-inductance of a straight dipole given in [10]. The bending of the wire introduced mutual capacitances between the adjacent wire segments that constitute a meander section. The mutual capacitance of a meander section is

$$C_m = \frac{\pi \epsilon_0 w}{ln\left[\frac{l_S}{a} + \sqrt{\left(\frac{l_S}{a}\right)^2 - 1}\right]} \tag{2}$$

where $l_S$ is the spacing between two parallel wires that form a meander section, $w$ is the width of the section, and $a$ is the radius of the wire

$$l_S = \frac{(l - 2wN)}{2(2N - 1)}. \tag{3}$$

Therefore, the resonant frequency $f_0$ of an MDA can be predicted as follows:

$$f_0 = \frac{1}{2\pi\sqrt{L_{31}\left(C_{31} + C_{32} + \frac{C_m}{2(2N-1)}\right)}} \tag{4}$$

where $N$ is the number of bends.

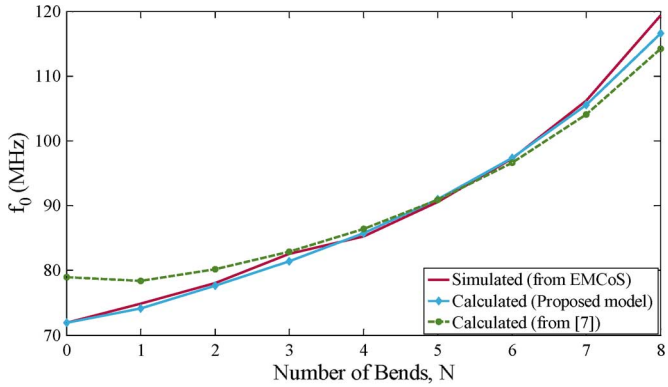


Fig. 4. Class-1 MDA. Resonant frequency $f_0$ as a function of the number of bends in one arm. Plot compares the results from numerical simulation in EMCoS and prediction from the frequency-independent, geometry-based MDA model. The length of the wire $L = 100$ cm, and width $w = 4.3$ cm.

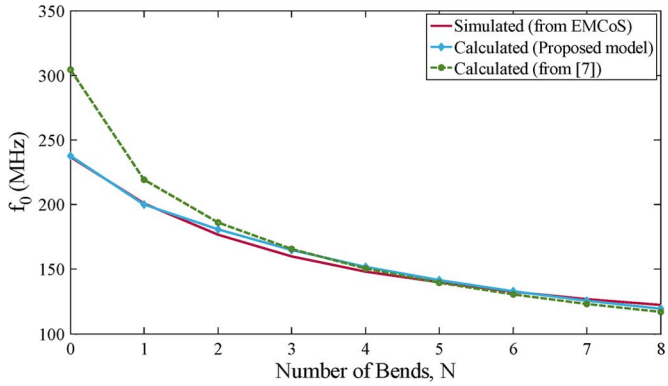


Fig. 5. Class-2 MDA. Resonant frequency $f_0$ as a function of the number of bends in one arm. Plot compares the results from numerical simulation in EMCoS and prediction from the frequency-independent, geometry-based MDA model. The height of the antenna above the ground plane $H = 30$ cm, and width $w = 4.3$ cm.

## III. Results and Analysis

To validate our model, both classes of meander dipole antennas were examined. A wire with a fixed length $L = 100$ cm, width $w = 4.3$ cm, and radius $a = 0.0525$ cm was chosen. Varying the number of bends, $N$ in a Class-1 MDA from zero to eight and comparing predictions of the resonant frequencies from (4) and [7] with numerical simulations in EMCoS [11], we obtain the result in Fig. 4. In comparing both predictions accurately, it is worth noting that a bend is defined differently in this letter than in [7], but there is a correlation given in (5). Let $N'$ represent the number of bends in an MDA as defined in [7] and $N$ be the number of bends as defined in our letter. Therefore, $N'$ is related to $N$ by

$$N' = 2N - 1. \tag{5}$$

The width of a section, $w$, is defined the same way in both works. In Fig. 4, there is good agreement between both models considered and the simulation results from $N = 3$ to $N = 7$, but a divergence could be observed below $N = 3$ and above $N = 7$. The largest deviations in the resonant frequency of our MDA model and [7] from the simulation results were 2.3% and 9.8%, respectively.

Similarly, for a Class-2 MDA, the height $H$ of each arm of the MDA was fixed at 30 cm while $w = 4.3$ cm. The number of bends was again varied from zero to eight. Resonant frequency predictions of our MDA model (4) and the inductive-circuit model [7] were compared to EMCoS simulation values and presented in Fig. 5. There is good agreement between both models considered with EMCoS simulation results for $N = 2$ and above. For $N = 2$ and below, the inductive-circuit model [7] deviated substantially, by up to 28% at $N = 0$. The largest deviation in the resonant frequency observed between our model and simulation results from $N = 0$ to $N = 8$ was 3.4%.

## IV. Radiation Resistance

The radiation resistance of an antenna is an integral part of characterizing the antenna in terms of its performance and efficiency. Therefore, we present an equation for estimating the

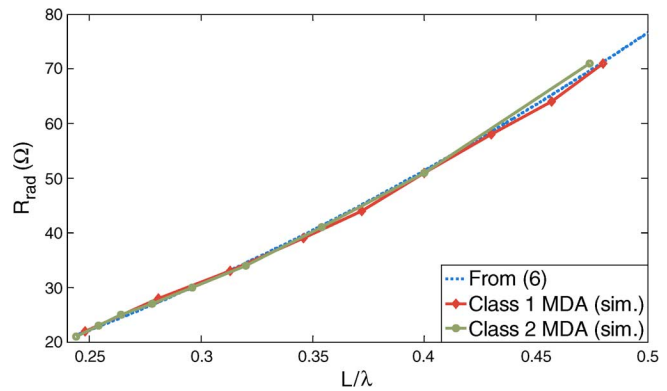


Fig. 6. Class-1 and Class-2 radiation resistances as a function of wavelength and predictions by (6). "sim." indicates that data was obtained by simulation in EMCoS.

resonant frequency of the MDA, which is a function of the geometry and frequency. This method considers the vertical segments of the MDA such as that shown in Fig. 3 as its main radiating elements. The input resistance of an MDA is given by

$$R_{\text{in}} = 34.15\left(2\pi\frac{(L-2wN)}{\lambda}\right)^{1.8} \tag{6}$$

where $L$ is the total length, i.e., both vertical and horizontal segments of each arm of the MDA, $w$ is the width, and $N$ is the number of bends. The input resistance equation in (6) was modeled after input resistance equations of dipoles in [12], but with the constants adapted to the MDA configuration. Assuming ohmic losses are negligible, the input resistance is the radiation resistance. An overlay of predicted radiation resistances on the values obtained via EMCoS [11] is contained in Fig. 6.

## V. Conclusion

An alternative model to characterize the resonant frequency and radiation resistance of a meander dipole antenna has been presented, and contrasts with existing models have been identified. The proposed model of an MDA, which is frequency-independent and based entirely on the geometry of the antenna, had been adapted from a model for straight dipole antennas [10]. The work described in this letter has produced an equation for

calculating the resonant frequency of an MDA, incorporating the mutual inductance between adjacent parallel wires formed through the process of bending the wire. Through analysis of the two possible "classes" of MDAs identified in the letter, the presented model has been validated due to a good agreement between the predicted [by (4)] and simulated resonant frequencies in Figs. 4 and 5. A discrepancy of less than 3% was observed for the various number of bends considered. An equation for calculating the radiation resistance of a meander dipole antenna that is a function of its geometry and frequency has been derived and presented. It is found to be consistent with prediction of radiation resistance from the EMCoS simulation tool. The proposed model is expected to be more broadband and versatile with the structure of the meander dipole antenna than existing models.

## REFERENCES

[1] J. Rashed and C.-T. Tai, "A new class of resonant antennas," *IEEE Trans. Antennas Propag.*, vol. 39, no. 9, pp. 1428–1430, Sep. 1991.

[2] G. Marrocco, "Gain-optimized self-resonant meander line antennas for RFID applications," *IEEE Antennas Wireless Propag. Lett.*, vol. 2, pp. 302–305, 2003.

[3] K. V. S. Rao, P. V. Nikitin, and S. F. Lam, "Antenna design for UHF RFID tags: A review and a practical application," *IEEE Trans. Antennas Propag.*, vol. 53, no. 12, pp. 3870–3876, Dec. 2005.

[4] H. Makimura, Y. Watanabe, K. Watanabe, and H. Igarashi, "Evolutional design of small antennas for passive UHF-band RFID," *IEEE Trans. Magn.*, vol. 47, no. 5, pp. 1510–1513, May 2011.

[5] D. K. C. Chew and S. R. Saunders, "Meander line technique for size reduction of quadrifilar helix antenna," *IEEE Antennas Wireless Propag. Lett.*, vol. 1, pp. 109–111, 2002.

[6] M. Ali and S. S. Stuchly, "A meander-line bow-tie antenna," in *IEEE AP-S Int. Symp. Dig.*, Jul. 21–26, 1996, vol. 3, pp. 1566–1569.

[7] T. Endo, Y. Sunahara, S. Satoh, and T. Katagi, "Resonant frequency and radiation efficiency of meander line antennas," *Electron. Commun. Jpn,*, vol. 83, no. 1, pt. II, pp. 52–58, Jan. 2000.

[8] S. R. Best and J. D. Morrow, "Limitations of inductive circuit model representations of meander line antennas," in *Proc. IEEE Antennas Propag. Soc. Int. Symp.*, Jun. 22–27, 2003, vol. 1, pp. 852–855.

[9] H. Nakano, H. Tagami, A. Yoshizawa, and J. Yamauchi, "Shortening ratios of modified dipole antennas," *IEEE Trans. Antennas Propag.*, vol. 32, no. 4, pp. 385–386, Apr. 1984.

[10] T. G. Tang, Q. M. Tieng, and M. W. Gunn, "Equivalent circuit of a dipole antenna using frequency-independent lumped elements," *IEEE Trans. Antennas Propag.*, vol. 41, no. 1, pp. 100–103, Jan 1993.

[11] EMCoS Antenna VLab. EMCoS, Ltd., Tbilisi, Georgia, 2011 [Online]. Available: http://www.emcos.com

[12] W. L. Stutzman and G. A. Thiele*, Antenna Theory and Design*. New York: Wiley, 1998, p. 171.